

# Supporting Information for "The Effect of Different Implementations of the Weak Temperature Gradient Approximation in Cloud Resolving Models"

N. Z. Wong<sup>1</sup>, Z. Kuang<sup>1,2</sup>

<sup>1</sup>Department of Earth and Planetary Sciences, Harvard University, Cambridge, MA, USA

<sup>2</sup>John A. Paulson School of Engineering and Applied Sciences, Harvard University, Cambridge, MA, USA

## Contents of this file

1. Figures S1
2. Figures S2
3. Figures S3
4. Figures S4

## Introduction

This supplementary contains four additional figures, a plot of the WTG approximation induced large-scale vertical velocity (Fig. S1), two time-series plots of daily-averaged hourly precipitation rates for full-radiative (Fig. S2) and idealised-radiative (Fig. S3) setups, and lastly a scatter plot similar to Fig. 2, but for different value of  $x$  in  $j^x$  that controls the response of the higher-order baroclinic modes in Spectral (SPC) scheme (Fig. S4)

## References

- Blossey, P. N., Bretherton, C. S., & Wyant, M. C. (2009, 3). Subtropical Low Cloud Response to a Warmer Climate in a Superparameterized Climate Model. Part II: Column Modeling with a Cloud Resolving Model. *Journal of Advances in Modeling Earth Systems*, 1(3), n/a-n/a. doi: 10.3894/JAMES.2009.1.8
- Herman, M. J., & Raymond, D. J. (2014, 12). WTG cloud modeling with spectral decomposition of heating. *Journal of Advances in Modeling Earth Systems*, 6(4), 1121–1140. doi: 10.1002/2014MS000359
- Kuang, Z. (2008, 2). Modeling the Interaction between Cumulus Convection and Linear Gravity Waves Using a Limited-Domain Cloud System-Resolving Model. *Journal of the Atmospheric Sciences*, 65(2), 576–591. doi: 10.1175/2007JAS2399.1
- Mlawer, E. J., Taubman, S. J., Brown, P. D., Iacono, M. J., & Clough, S. A. (1997, 7). Radiative transfer for inhomogeneous atmospheres: RRTM, a validated correlated-k model for the longwave. *Journal of Geophysical Research: Atmospheres*, 102(D14), 16663–16682. doi: 10.1029/97JD00237
- Pauluis, O., & Garner, S. (2006, 7). Sensitivity of Radiative-Convective Equilibrium Simulations to Horizontal Resolution. *Journal of the Atmospheric Sciences*, 63(7), 1910–1923. doi: 10.1175/JAS3705.1
- Raymond, D. J., & Zeng, X. (2005, 4). Modelling tropical atmospheric convection in the context of the weak temperature gradient approximation. *Quarterly Journal of the Royal Meteorological Society*, 131(608), 1301–1320. doi: 10.1256/qj.03.97

Copyright 2023 by the American Geophysical Union.  
0094-8276/23/\$5.00

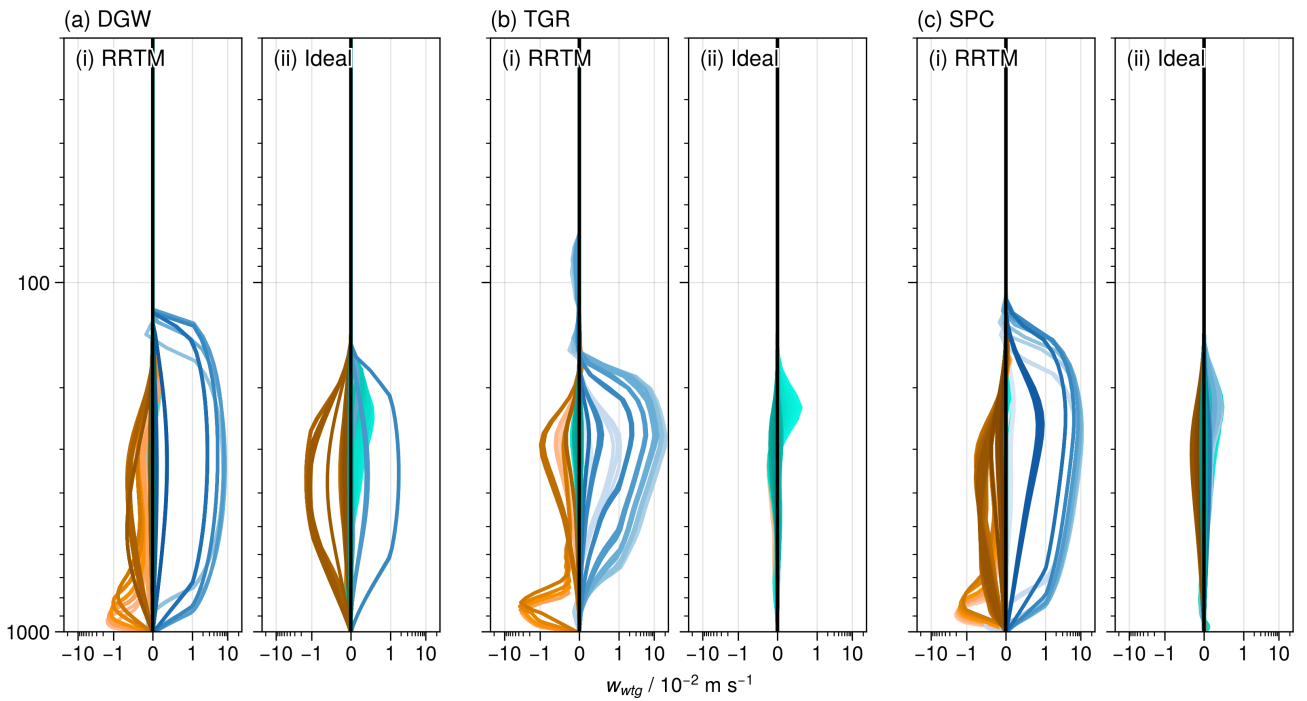


**Figure S1.** We plot the time-averaged WTG-induced large-scale vertical velocity for the (a) Damped Gravity Wave (DGW, Kuang (2008); Blossey et al. (2009)), (b) Temperature Gradient Relaxation (TGR, Raymond and Zeng (2005)) and (c) Spectral (SPC, Herman and Raymond (2014)) Weak Temperature Gradient implementations respectively, for the (i) RRTM radiation and (ii) idealised-radiative cooling schemes respectively. We see that the TGR implementation results in the most top- and bottom-heavy vertical structures, while the DGW implementation results in the least, and the SPC implementation is somewhere in the middle. This is consistent with the response of higher-order baroclinic modes being weakest and strongest in the DGW and TGR implementations respectively.

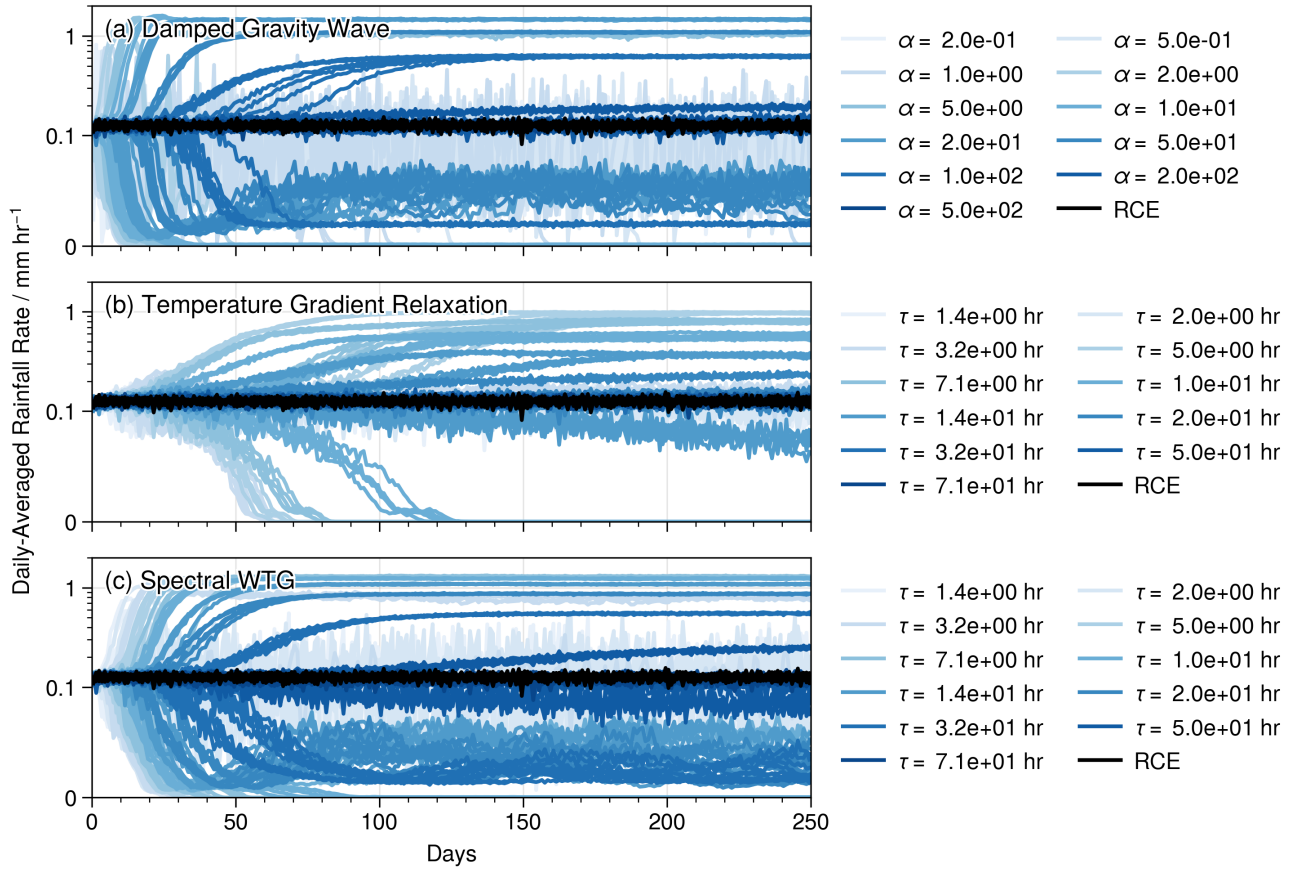


**Figure S2.** We plot the time-series of daily-averaged hourly precipitation rate for the (a) Damped Gravity Wave (Kuang, 2008; Blossey et al., 2009), (b) Temperature Gradient Relaxation (Raymond & Zeng, 2005) and (c) Spectral (Herman & Raymond, 2014) schemes. Here, we see that when the radiative scheme is interactive (we used the RRTM radiation scheme of Mlawer et al. (1997)), all models will enter a multiple-equilibria regime with wet and dry steady states as the implementation strength increases ( $\alpha \sim O(10)$ ,  $\tau \sim O(5 \text{ hr})$ ). Eventually however, as the implementation strengths increase further ( $\alpha < 1$ ,  $\tau \leq 1 \text{ hr}$ ), the steady states collapse into an oscillatory regime reminiscent of convectively-coupled waves.

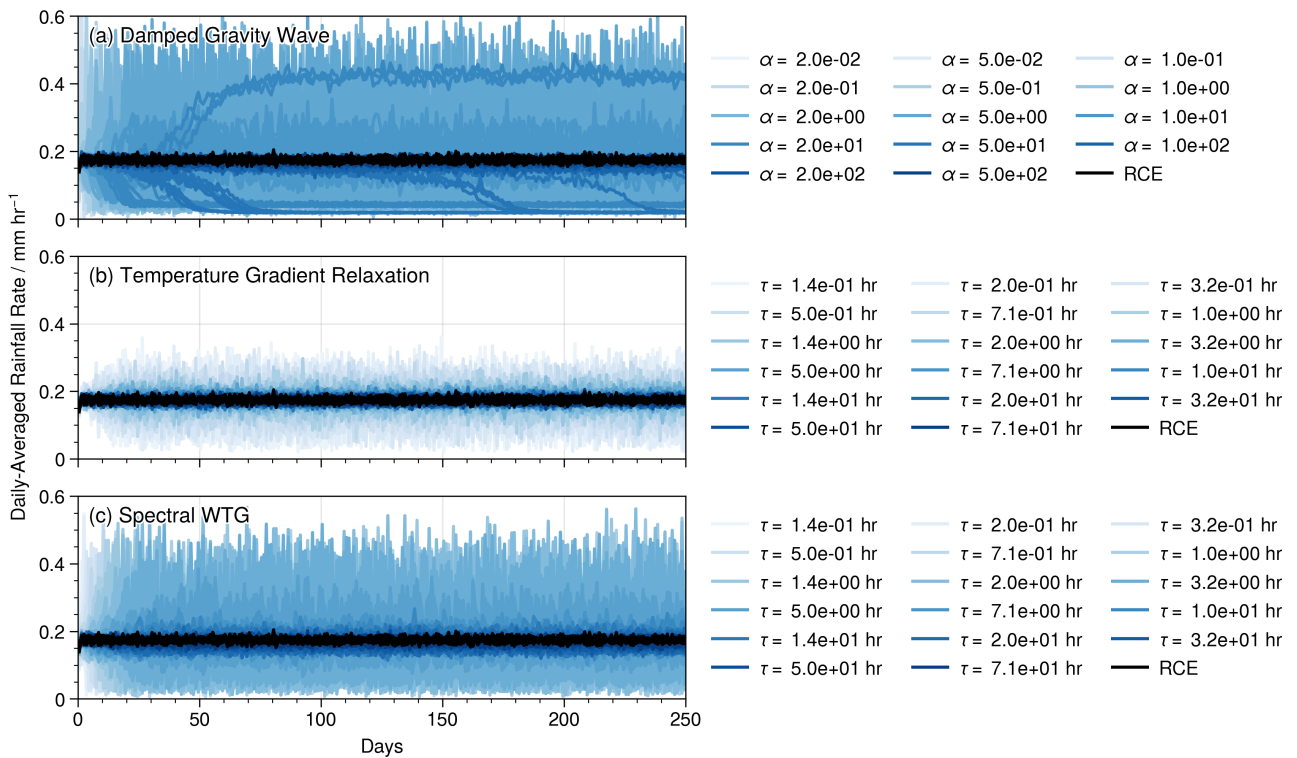


**Figure S3.** Similar to Fig. S2, except this time for the idealised radiative scheme of Pauluis and Garner (2006). We see that the multiple-equilibria regime only appears in the (a) Damped Gravity Wave (DGW) scheme ( $\alpha \sim O(20)$ ). However, we see that the (c) Spectral (SPC) scheme also transitions into an oscillatory state similar to the DGW implementation when the implementations are strong enough ( $\alpha < 10$ ,  $\tau < 5$  hr). However, the oscillatory regime does not appear when the Temperature Gradient Relaxation implementation until the strength of the implementation is close to being unphysical (i.e.  $\tau < 0.2$  hr, note how light the colours are in (b) where the oscillatory behaviour is significant compared to the DGW and SPC schemes).

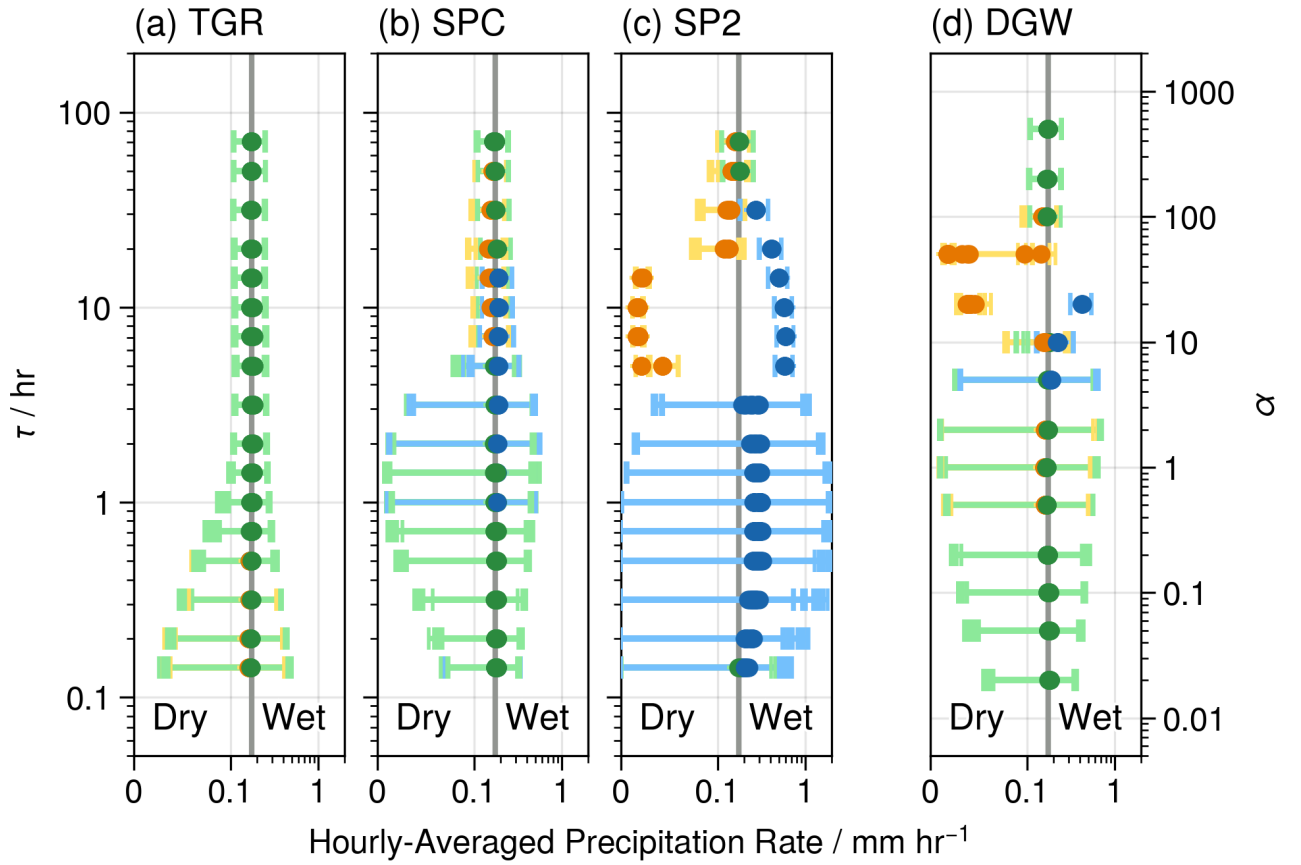


**Figure S4.** Domain-mean hourly-averaged precipitation rate  $P_{WTG}$  for the (a) Temperature Gradient Relaxation (TGR, Raymond and Zeng (2005)) and (b) Spectral (SPC, Herman and Raymond (2014)) Weak Temperature Gradient implementation, (c) 2nd-order Spectral (SP2) Weak Temperature Gradient implementation and the (d) Damped Gravity Wave (DGW, Kuang (2008); Blossey et al. (2009)) implementation respectively, under the idealised-radiative cooling scheme of Pauluis and Garner (2006). We see that the 2nd-order Spectral (SP2) implementation shows a stronger bifurcation than the 1st-order Spectral (SPC) implementation, showing that the strength of the multiple-equilibria and the oscillatory regimes increases as the strength of the higher-order baroclinic modes decreases.